Macromolecules
NOTE

Macromolecules **2009**, *42*, 9609–9612 **9609**
DOI: 10.1021/ma9021357

Easy Orientation of Diblock Copolymers on Self-Assembled Monolayers Using UV Irradiation

Pang-Hung Liu, Pascal Thébault, Patrick Guenoun, and Jean Daillant*

CEA, IRAMIS, LIONS, CEA-Saclay, F-91191 Gif-sur-Yvette Cedex, France

Received February 12, 2009; Revised Manuscript Received October 26, 2009

The control of the surface energy of self-assembled monolayers (SAMs) for orientating diblock copolymer mesophases has been achieved using different methods. The goal is usually to obtain a neutral surface, that is, a surface exhibiting similar interfacial energies with both blocks of the copolymer in order to promote perpendicular orientation. Historically, the first method to be used was to spin-coat random copolymers made of the same monomers on the substrate,[1] as different surface energies can be achieved by varying the ratios of monomers in synthesis. Further, a major improvement was to modify the random copolymer at one end with a chemical group which could be grafted on the surface in order to prevent the random copolymer to dewet or diffuse in the block copolymer.[2,3] Besides this surface specific chemistry, cross-linking on the random copolymer has also recently been used to increase the film stability.[4] More recently, the thickness dependence of the orientation has been investigated,[5] and it has been shown that the formation of perpendicular domains on a random copolymer brush needs to be viewed in terms of the equilibration of the block copolymer and the random copolymer in the presence of each other and not simply in terms of interfacial energy.[6]

A different strategy has been to use self-assembled monolayers (SAM) like octadecyltrichlorosilane (OTS). However, though it has been shown that 3-(*p*-methoxyphenyl)propyltrichlorosilane could provide neutral surfaces for PS-*b*-PMMA (polystyrene−poly(methyl methacrylate)) on a silicon wafer,[7] such monolayers usually do not have the right surface energy, and different methods have been used in order to control this energy. It has for example been shown that incomplete OTS monolayers could also be used.[8] Whereas this method is extremely versatile, it leads to a necessarily heterogeneous film which might prevent control at very small scales. Another possibility is irradiation of SAMs with synchrotron soft X-rays[9,10] or treatment with CO_2 plasma.[11] Oxidation through ultraviolet (UV) radiation has also been recently used to produce wettability gradients.[12] In this paper we show that UV irradiation indeed provides a versatile tool to precisely tune the surface energy of a SAM. We show in particular that the orientation of PS-*b*-PMMA lamellar and cylinder phases can be controlled using this method.

Si wafers (p-type, boron doped, 250 μm thick) were first cleaned by sonication in purified Millipore water (resistivity 18 MΩ·cm), 1:1 water/ethanol mixture, chloroform, and heptane, followed by piranha treatment (1/3 v/v of 30% H_2O_2/98% H_2SO_4) at 80 °C and exposure to UV under an oxygen atmosphere for 30 min. The cleaned wafers were rinsed with purified water, dried with nitrogen, and silanized in a 2 mM solution of OTS in heptane for 1 day. The reaction of OTS with oxidized silicon wafers proceeds first by hydrolysis of the labile Cl groups of the OTS molecule into hydroxyl groups by the small amount of water present in heptane. Then, condensation to oligomers occurs followed by bonding to the silanol groups of the substrate.[13] The wafers were then sonicated in chloroform and purified water and dried with nitrogen before UV/ozone treatment.

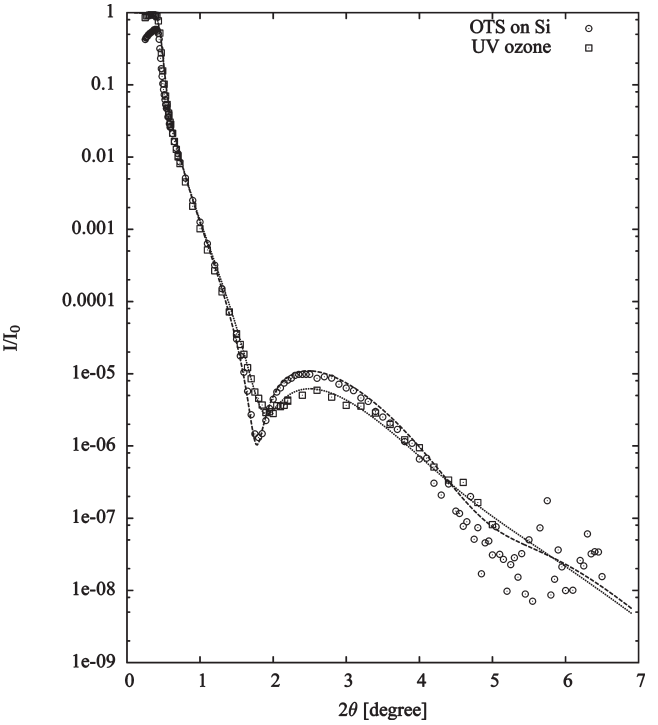

Figure 1. Reflectivity results of a typical OTS layer (circle) and a 6 min UV ozone-treated OTS layer with the calculated curves (dashed line and dotted line, respectively).

The silanized wafers were then exposed to UV light (185 and 254 nm) in an oxygen-filled chamber at a distance of 4 cm from the lamp, for specific time periods, rinsed with purified water and chloroform, and dried with nitrogen.

The OTS layers were first characterized using X-ray reflectivity using a Siemens powder diffractometer D5000 operated with a homemade software. The Cu Kα is first collimated using 50 μm slits. A graphite monochromator is placed after the sample in front of the NaI scintillator detector. The homemade software allows one to record rocking curves at each point of the reflectivity curve in order to subtract the background. The reflectivity curves before and after UV treatment are given in Figure 1. X-ray reflectivity curves were fitted using the IMD extension of the XOP package using the classical Parratt

*To whom correspondence should be addressed. E-mail: Jean.Daillant@cea.fr.

Published on Web 11/16/2009

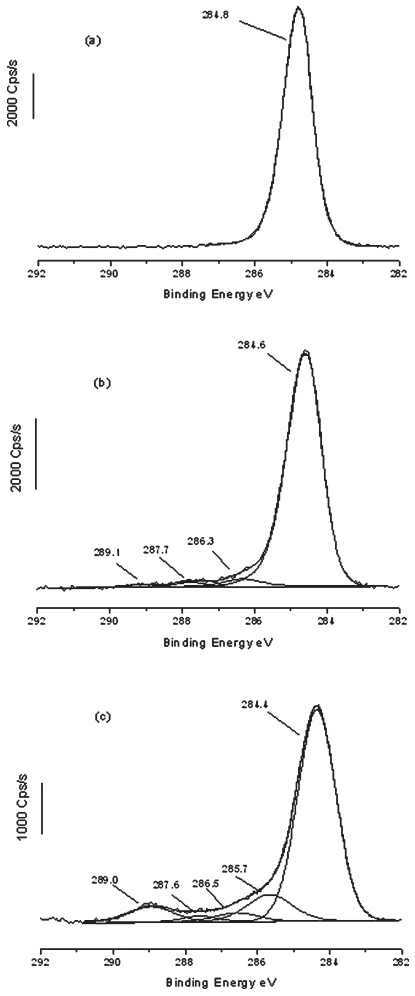

Figure 2. High-resolution XPS spectra of the C 1s region of an OTS-coated Si wafer (a), after 5 min of UV/ozone treatment (b), and after 30 min of UV/ozone treatment (c).

formalism. We used a two-box model with one box of constant electron density for describing the $C_{18}H_{37}$ OTS chains and another one for the Si headgroups. Each box is limited by two rough interfaces described using an error function profile characterized by its rms roughness. Best fit of the reflectivity curve to this model yields a substrate roughness of 0.4 nm, an OTS layer thickness of 2.45 nm, and an OTS layer−air roughness of 0.65 nm, in good agreement with ref 14. After 6 min UV ozone treatment, the thickness of the OTS layer decreases to 2.27 nm whereas its roughness increases to 0.785 nm, indicating changes in the top surface structure and composition. Attempts to add a specific surface layer to the model did not lead to significantly better fits.

In order to better understand the surface chemistry of UV irradiation, XPS analyses were performed using a Kratos Axis-Ultra DLD spectrometer, using the monochromatized Al Kα line at 1486.6 eV with a power source of 150 W. Fixed analyzer pass energy of 20 eV was used for all core level scans. The photoelectron takeoff angle was 90° with respect to the sample plane, which provides an integrated sampling depth of ~15 nm. The analyzed surface was 700 μm × 300 μm. Binding energies were calibrated against the Au $4f_{7/2}$ binding energy of a gold surface at 83.90 eV.

Figure 2 shows high-resolution XPS spectra of the C 1s core level peaks corresponding to OTS-coated Si wafers (Figure 2a), after 5 min of UV/ozone treatment (Figure 2b), and after 30 min of UV/ozone treatment (Figure 2c). The C 1s peak, of the OTS surface, was best fitted with one peak at 284.8 eV corresponding to the carbon in C−C and C−H bonds.[15] After 5 min of UV/ozone, we observe the apparition of three new peaks. The first peak, at the lowest binding energy of 286.3 eV, is assigned to the carbon atoms in C−OH bonds (hydroxyl groups), the second peak at 287.7 eV is attributed to the carbon atoms in O═C−H bonds (aldehyde groups), and the third peak at 289.1 eV is assigned to the carbon atoms in HO−C═O bonds (acidic carboxylic groups).[16,17] After 30 min of UV/ozone treatment, we observe an increase in the component at 289.0 eV and the apparition of a peak at 285.7 eV corresponding to the carbon atoms in α position of acidic groups, which cannot be visible before due to the small amount of acidic groups. We also observed a decrease of C−C area peak with the increase of UV/ozone irradiation time which is attributed to the formation of oxidized carbons and a likely break of C−C bonds. After a longer time of UV/ozone (spectra not shown), we observe a complete disappearence of the OTS layer. This XPS study shows UV/ozone oxidation of OTS layers, first by hydroxyl and aldehyde groups formation then by carboxylic acid groups formation. These results can be connected to the contact angle measurements which shows an increase in hydrophilicity with increasing UV/ozone irradiation times.

Table 1. Equilibrium Angle, Advancing Angle, Receding Angle, and Hysteresis for Water on UV-Treated OTS Wafers as a Function of the Irradiation Time

UV irradiation time (min)	equilibrium angle (deg)	advancing angle (deg)	receding angle (deg)	hysteresis (deg)
OTS	111.5	114.4	101.0	13.4
5	78.3	86.1	72.9	13.2
7	74.6	77.0	65.1	11.9
9	71.0	73.0	56.7	16.3

Contact angle measurements were performed according to the sessile drop method using a Dataphysics OCA20 contact angle system at room temperature. The volume of the water droplets used for the measurements was 3.0 μL. All reported contact angles are the average of three measurements taken at different locations of the wafer. Advancing and receding contact angles for water as well as the contact angle hysteresis on the order of 10° are given in Table 1. More precisely, the surface energy of solid surfaces is usually characterized through so-called Zisman plots which consist of plotting the cosine of the contact angle θ of an homologous series of liquids as a function of the liquid surface tension γ of the liquid (Figure 3a).[18,19] The intercept at $\cos\theta = 1$ gives the critical surface tension of the surface γ_C, which indicates whether a given liquid will wet ($\gamma < \gamma_C$) or not ($\gamma > \gamma_C$) the substrate. In principle, nonpolar homologous liquids like alkanes should be used, but in practice this also works very well even with water.[20] From fitting the Zisman plots for tetradecane, hexadecane, squalane, bicyclohexyl, diiodomethane, and purified water (Figure 3a), we obtain the critical surface tensions shown in Figure 3b.The critical surface energies range from 19.6 mN/m for the native surface layer, in good agreement with literature,[21] to 27.7 mN/m after 8 min UV irradiation, demonstrating that our method allows a very precise control of the surface energy, down to a fraction of a mN/m. In order to characterize the surface independently of our irradiation time (a parameter which may vary from an apparatus to another), we report in Figure 3b the critical surface tension as a function of the water contact angle. This parameter is very sensitive to the oxidation state of the surface. A very smooth and linear variation is then obtained over a range of angles very similar to the one found by Han et al.[6]

Diblock copolymers of PS_{52K}-*b*-$PMMA_{52K}$ (PDI: 1.09) of symmetric composition and PS_{46K}-*b*-$PMMA_{21K}$ (PDI: 1.09) of asymmetric composition were purchased from Polymer Source Inc. PS_{52K}-*b*-$PMMA_{52K}$ exhibits a lamellar phase of period

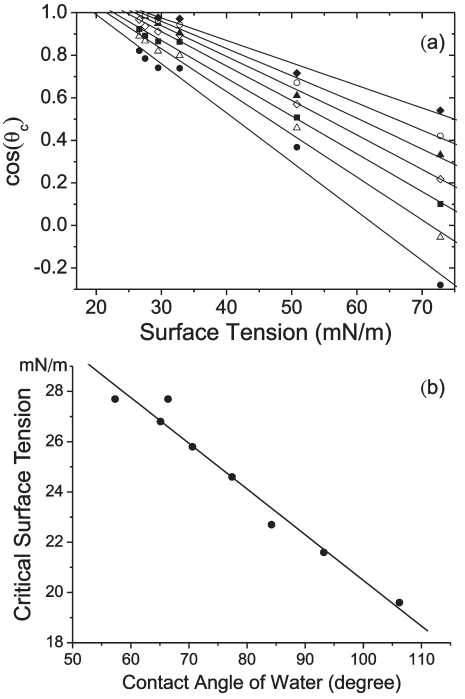

Figure 3. (a) Zisman plots, cosine of the contact angle cos θ_c as a function of the surface tension of tetradecane, hexadecane, squalane, bicyclohexyl, diiodomethane, and purified water (from left to right in increasing order) on silanated wafers treated with different UV/ozone time periods: native wafer (filled circles), 3 min (open triangles), 4 min (filled squares), 5 min (open diamonds), 6 min (filled triangles), 7 min (open circles), 9 min (filled diamonds). (b) Critical surface tensions as determined by the intercepts of the curves in (a) as a function of water contact angle. The latter angle is chosen as a sensitive characteristic parameter of the surface.

L_0 = 49 nm in the bulk, as determined in ref 22, whereas PS_{46K}-*b*-$PMMA_{21K}$ exhibits a phase of PMMA cylinders (of about 36 nm for the center to center spacing) in PS. 1 wt % solutions of PS_{52K}-*b*-$PMMA_{52K}$ and PS_{46K}-*b*-$PMMA_{21K}$ in toluene were spin-coated onto silanized silicon wafers treated with UV/ozone at 2000 and 2500 rpm to produce copolymer films with thicknesses ca. 34 and 31 nm, respectively. Subsequently, the samples were annealed in a vacuum oven of pressure less than 3 kPa at 170 °C for 1 day.

Atomic force microscopy (AFM, Digital Instruments, Nanoscope V) was employed in tapping mode for imaging PS-*b*-PMMA films at room temperature. AFM images were taken at different locations on the substrate and show that the orientation is homogeneous over the entire surface. Phase images allow one to easily distinguish PS (dark) from PMMA (bright) domains.[23] After spin-coating, due to low surface energies, no copolymer was observed on nontreated (γ_C = 19.6 mN/m) and 3 min UV/ozone-treated (γ_C = 21.6 mN/m) samples. For the samples with water contact angles of 87° and 84°, dewetting can be observed under optical microscopy and AFM (insets of Figure 4a,f). As shown in Figure 4a−e, perpendicular orientation of the lamellar phase of the PS_{52K}-*b*-$PMMA_{52K}$ copolymer is obtained on the samples with γ_C from 23.9 to 25.7 mN/m. Its period is ca. 50 nm as expected from bulk studies. Figure 4f−j shows the different morphogies obtained after UV/ozone treatment for the PS_{46K}-*b*-$PMMA_{21K}$ copolymer films. First, on the sample with γ_C = 22.7 mN/m, dewetting of copolymer is observed after annealing (Figure 4f). Perfect perpendicular orientation of the cylinders is obtained after 5 min UV/ozone treatment (Figure 4g, γ_C = 24.6 mN/m). From the FFT of AFM images, the average distance between them is 33 nm. After 6 min (Figure 4h, γ_C = 25.8 mN/m), the phase contrast is obviously much reduced and the

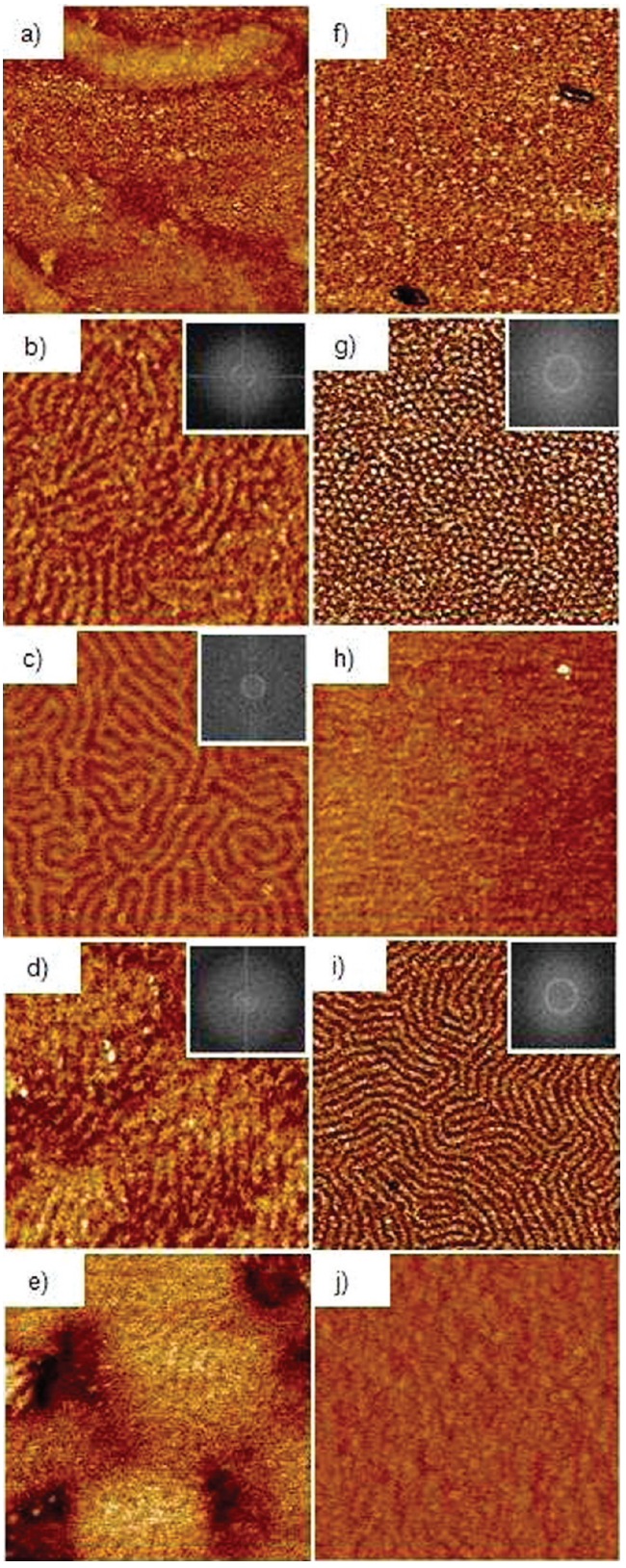

Figure 4. Tapping-mode AFM phase images of (a−e) 34 nm thick PS_{52K}-*b*-$PMMA_{52K}$ and (f−j) 31 nm thick PS_{46K}-*b*-$PMMA_{21K}$ films on OTS layers treated with UV/ozone for water contact angles of (a) 87°, (b) 80°, (c) 77°, (d) 70°, (e) 62°, (f) 84°, (g) 77°, (h) 71°, (i) 65°, and (j) 57°. The image size is 1.0 × 1.0 μm^2. Insets show the FFTs of the images which exhibit structures. The difference between the lamellar phase and the cylindrical phase is clearly visible.

Table 2. Results of Contact Angles, Critical Surface Energies, and the Phases Observed in AFM Images

sample	$\theta_{C,water}$ (deg)[a]	γ_C (mN/m)[b]	description[c]
C1	84	22.7	
C2	77	24.6	$C_\perp$
C3	71	25.8	
C4	65	26.8	$C_\parallel$
C5	57	27.7	
L1	87	22.7[d]	dewetting
L2	80	23.9[d]	$L_\parallel$
L3	77	24.5[d]	$L_\parallel$
L4	70	25.7[d]	$L_\parallel$
L5	62	27.1[d]	dewetting

[a] Contact angles of water in degrees. [b] Critical surface energy values in mN/m. [c] The phases or morphology observed in AFM images. [d] Values calculated from linear interpolation of $\theta_{C,water}$.

orientation is lost. After 7 min treatment, elongated stuctures are observed (Figure 4i, γ_C = 26.8 mN/m). The structure gives a spacing of 39 nm, which is close to the value of 33 nm $\times$ $2/\sqrt{3}$. This indicates that they should be the same cylindrical structure observed on 5 min treated sample but lie flat on the surface. Finally, after 8 and 9 min treatment (Figure 4j, γ_C = 27.7 mN/m) this orientation is lost again.

Perpendicular orientation of the lamellar phase was obtained for a wide range of thicknesses from 30 to 55.5 nm. For much thicker films of 80 nm no orientation was observed. Our technique is therefore nicely complementary to Ham's method[5] since it also allows the orientation of thicker films. We have also checked the same behavior, for the cylindrical phase, where perpendicular orientation has been obtained for 31, 36, and 42 nm thick films.

One puzzling question is the discrepancy between the optimal critical surface tensions we find for perpendicular orientation and expectations from PS and PMMA surface tensions. According to the literature, the surface tensions of PS and PMMA at our annealing temperature of 170 °C are $\gamma_{PS} \approx 29.7-29.9$ mN/m and $\gamma_{PMMA} \approx 29.9-31$ mN/m, respectively.[2,24,25] If we assume that the neutral surface would have a surface energy of ≈29.9 mN/m, then this would be ≈ 5 mN/m more than the corresponding critical surface tension of 24.5 mN/m. Such a difference has been noticed for polyethylene in ref 24, for which, at 20 °C, the critical surface tension is found to be ≈5 mN/m smaller than the surface energy.

In this paper, we have demonstrated that UV/ozone oxidation of OTS layers provides a simple and versatile way of controlling the orientation of block copolymers through a precise control of the surface energy. We have shown by XPS that the UV/ozone treatment leads to oxidation of OTS layers, first by hydroxyl and aldehyde groups formation and then by carboxylic acid groups formation and a likely break of C−C bonds. The slight increase in oxidation with the increasing UV/ozone irradiation times allows for this precise control of the surface energy.

Acknowledgment. Pang-Hung Liu and Pascal Thébault gratefully acknowledge support form the "Chimtronique" program of CEA. The authors also gratefully thank O. Taché et C. Blot for support during the X-ray experiments.

References and Notes

(1) Kellogg, G. J.; Walton, D. G.; Mayes, A. M.; Lambooy, P.; Russell, T. P.; Gallagher, P. D.; Satija, S. *Phys. Rev. Lett.* **1996**, *76*, 2503–2506.
(2) Mansky, P.; Liu, Y.; Huang, E.; Russell, T. P.; Hawker, C. J. *Science* **1997**, *275*, 1458–1460.
(3) Huang, E.; Russell, T. P.; Harrison, C.; Chaikin, P. M.; Register, R. A.; Hawker, C. J.; Mays, J. W. *Macromolecules* **1998**, *31*, 7641–7650.
(4) Ryu, D. Y.; Wang, J.-Y.; Lavery, K. A.; Drockenmuller, E.; Satija, S. K.; Hawker, C. J.; Russell, T. P. *Macromolecules* **2007**, *40*, 4296–4300.
(5) Ham, S.; Shin, C.; Kim, E.; Ryu, D. Y.; Jeong, U.; Russell, T. P.; Hawker, C. J. *Macromolecules* **2008**, *41*, 6431–6437.
(6) Han, E.; Stuen, K. O.; La, Y.-H.; Nealey, P. F.; Gopalan, P. *Macromolecules* **2008**, *41*, 9090–9097.
(7) Park, D.-H. *Nanotechnology* **2007**, *18*, 355304.
(8) Niemz, A.; Bandyopadhyay, K.; Tan, E.; Cha, K.; Baker, S. M. *Langmuir* **2006**, *22*, 11092–11096.
(9) Kim, T. K.; Yang, X. M.; Peters, R. D.; Sohn, B. H.; Nealey, P. F. *J. Phys. Chem. B* **2000**, *104*, 7403–7410.
(10) Peters, R. D.; Yang, X. M.; Kim, T. K.; Sohn, B. H.; Nealey, P. F. *Langmuir* **2000**, *16*, 4625–4631.
(11) Delorme, N.; Bardeau, J.-F.; Bulou, A.; Poncin-Epaillard, F. *Thin Solid Films* **2006**, *496*, 612–618.
(12) Smith, A. P.; Sehgal, A.; Douglas, J. F.; Karim, A.; Amis, E. J. *Macromol. Rapid Commun.* **2003**, *24*, 131–135.
(13) Ulman, A. *Chem. Rev.* **1996**, *96*, 1533–1554.
(14) Tidswell, I. M.; Ocko, B. M.; Pershan, P. S.; Wasserman, S. R.; Whitesides, G. M.; Axe, J. D. *Phys. Rev. B* **1990**, *41*, 1111–1128.
(15) Jiang, P.; Li, H. S.-Y.; Sugimura; Takai, O. *Appl. Surf. Sci.* **2006**, *252*, 4230–4235.
(16) Bain, C.; Troughton, E.; Tao, Y.-T.; Evall, J.; Whitesides, G.; Nuzzo, R. *J. Am. Chem. Soc.* **1989**, *111*, 321–335.
(17) Caro, A.; Humblot, V.; Methivier, C.; Minier, M.; Salmain, M.; Pradier, C.-M. *J. Phys. Chem. B* **2009**, *113*, 2101–2109.
(18) de Gennes, P. G. *Rev. Mod. Phys.* **1985**, *57*, 827–863.
(19) Zisman, W. Contact Angle, Wettability and Adhesion. In *Advances in Chemistry Series*; Fowkes, F. M., Ed.; American Chemical Society: Washington, DC, 1964; Vol. *43*, p 1.
(20) van Giessen, A.; Bukman, D.; Widom, B. *J. Colloid Interface Sci.* **1997**, *192*, 257–265.
(21) Brzoska, J. B.; Ben Azouz, I.; Rondelez, F. *Langmuir* **1994**, *10*, 4367–4373.
(22) Stoykovich, M.; Muller, M.; Kim, S.; Solak, H.; Edwards, E.; de Pablo, J.; Nealey, P. *Science* (*Washington, D.C.*) **2005**, *308*, 1442–1446.
(23) Magonov, S.; Reneker, D. *Annu. Rev. Mater. Sci.* **1997**, *27*, 175–222.
(24) Wu, S. *J. Phys. Chem.* **1970**, *74*, 632–638.
(25) Chee, K. *J. Appl. Polym. Sci.* **1998**, *70*, 697–703.